Inductive multi-proxy analysis of Mesolithic demographics on the Norwegian Skagerrak coast

Isak Roalkvam

University of Oslo, Institute of Archaeology, Conservation and History

04 October, 2022

1 Introduction

Population size is regarded as one of the primary drivers of cultural variation, and is of critical importance to our understanding of past human societies (Shennan, 2000). The frequency distribution of radiocarbon dates has been used extensively as one proxy for past relative population sizes (e.g. Crema, 2022; French et al., 2021), including in Norwegian Stone Age archaeology (Bergsvik et al., 2021; Jørgensen et al., 2020; Lundström et al., 2021; Nielsen, 2021; Nielsen et al., 2019; Solheim, 2020; Solheim and Persson, 2018). The potentially immense value of insights into past population dynamics, combined with the ubiquity of radiocarbon dates and the relative ease with which these can now be processed within what has been termed a dates as data methodology has undoubtedly contributed to the popularity of the approach. Several limitations and forms of criticism have, however, been directed at these procedures. Some of the objections are of a methodological nature, while others pertain to the underlying logic and the degree to which there is likely to be a direct connection between the frequency of ^{14}C-dates and population dynamics (Carleton and Groucutt, 2021; Torfing, 2015). What appears to be agreed upon by practitioners and critics alike is that radiocarbon dates are best analysed in this manner when compared and contrasted to other proxies for past population dynamics and other variables that might impact these (French, 2016; Palmisano et al., 2017). This paper reports on and attempts to unpack the relationship between two measures that have been linked to relative population size in the context of the Mesolithic Skagerrak coast in south-eastern Norway, namely summed probability distribution of calibrated radiocarbon dates and the summed probability distribution of shoreline dated sites (hereafter RSPD and SSPD, respectively).

2 Background

Large parts of the post-glacial landscape of Northern Scandinavia is characterised by dramatic isostatic uplift that has led to a net sea-level fall throughout the Holocene, despite eustatic sea-level rise (e.g. Mörner, 1979). As coastal foragers appear to have predominantly settled on or close to the contemporaneous shoreline, this can be utilised to assign an approximate date to the sites. This is done by coupling the present-day altitude of the sites with reconstructions of past shoreline displacement—a method known as shoreline dating. This is not least useful for dating the large number of surveyed sites in the region where other temporal data that often follow with an excavation are not available, such as radiocarbon dates or typological indicators in artefact inventories.

The frequency of shoreline dated sites has also been compared to RSPDs in the past (Solheim et al., 2018; Tallavaara and Pesonen, 2020). However, this has been done by finding point estimates of shoreline dates that are then aggregated in somewhat arbitrary bins of 200 or 500 years. This therefore does not take into account the uncertainty in the distance between the sites and the contemporaneous shoreline, nor the impact the variability in the rate of sea-level change has on the precision of the dates that can be achieved with the

method. In a recent study, Roalkvam (2022) has presented a probabilistic method for shoreline dating that takes these parameters into account, thus setting the stage for a more refined investigation of the relationship between frequency of ^{14}C-dates and shoreline dated sites. The parametrisation of the method is based on simulating the distance between sites with ^{14}C-dates and the prehistoric shoreline along the Skagerrak coast between Horten municipality in the northeast to Arendal municipality in the southwest (see map in Figure 1). The results of this indicate that the sites tend to have been located close to the shoreline until just after 4000 BCE when a few sites become more withdrawn from the shoreline, followed by a clear break around 2500 BCE, at which point shoreline dating appears to loose its utility. Thus, these geographical and temporal limits are also used for this study.

The title of this paper includes the word 'inductive' to indicate that while some speculative thoughts concerning the relationship between the above-outlined variables underlie the analysis, these could not be instantiated as concrete hypotheses. The data have thus been explored using a wide range of techniques in an attempt to unpick patterns and grasp the relationship between the variables. The dates as data approach is dependent on there being a direct link between the past generation of material that ultimately become ^{14}C samples and population size. The sum of shoreline dated sites, on the other hand, is determined by site frequency, and if used as a proxy for population size is therefore dependent on there being a connection between site count and population size. If a comparison of these proxies do not or only partially correspond, it is thus an open question what factors have impacted either distribution to cause this discrepancy, and which measure, if any, reflect true population dynamics. The issue will therefore initially demand an open and exploratory approach where a multitude of explanatory and confounding effects can be drawn on to explain any observed pattern.

To what degree the radiocarbon record is determined by past population numbers might vary both geographically and chronologically, based on variation in investigatory and taphonomic factors (Bluhm and Surovell, 2019; Surovell et al., 2009), as well as cultural processes within prehistoric populations. One example of the latter is the difference that might exist between farmer and forager populations, where Freeman et al. (2018) have suggested that an increased per capita energy consumption introduced with farming means that ^{14}C-dates should not be weighted equally when making relative population estimates across such populations. Similarly, while site counts have also been invoked for the analysis of past population dynamics, these are likely to be impacted by factors such as settlement nucleation and dispersion, as well as land-use and mobility patterns (Palmisano et al., 2017). However, these could be considered theoretical issues that have implications for how fluctuations in these proxies should be interpreted. Before any such fluctuations are given any substantive interpretation, however, there are a host of methodological issues that have to be considered.

The most critical of these follow from the fact that the summation of the probabilities associated with the dates for the SPDs is not a statistically coherent procedure. This is because the summed probabilities can no longer been seen as probabilities but is rather the combination of events and uncertainties, making the two indistinguishable, and rendering the interpretation of the resulting sum difficult (Blackwell and Buck, 2003; Crema, 2022). As Timpson et al. (2021, p. 2) put it: 'the SPD is not *the* single best explanation of the data, nor even *a* explanation of the data, but rather a conflation of many possible explanations simultaneously, each of which is mired by the artefacts inherited from the calibration wiggles.' The SPD is not a model. It is the combined representation of a range of possible explanations for the data—the frequency of dated events combined with the variable uncertainty associated with these (Carleton and Groucutt, 2021). This means that an SPD cannot be used directly to draw inferences on population dynamics, nor can it be directly compared to other time-series data (Carleton et al., 2018). While this problem can never be entirely resolved, a range of approaches have been developed in an attempt to work around this issue.

The most commonly applied of these is a null-hypothesis significance testing approach by means of Monte Carlo simulation, as introduced by (Shennan et al., 2013"). This works by comparing the observed RSPD with a series of simulated RSPDs generated from a null-model. These null-models are typically a exponential or logistic model, fit to the observed RSPD by means of regression, or a uniform model. The result from these simulations are then used to create a 95% critical envelope representing the null model. The proportion of the observed RSPD that falls outside this envelope is then used to estimate a p-value indicating whether the null model can be rejected. In the case that it can, the portions of the observed RSPD that falls outside this envelope can subsequently be interpreted as representing potentially meaningful demographic events, relative to the null model. However, care has to be taken in how these should be interpreted and inferential modesty

is called for (Timpson et al., 2021). First, this follows from the fact that 5% of the deviations from the critical envelope can be expected to be random, and there is no way to know which deviations this pertains to. Secondly, the p-value only indicates whether or not the null model can be rejected as an explanation of the data, and does not provide statistical justification for interpreting the deviations themselves as meaningful demographic signals. Finally, a for example exponential null model fit to the data is only one of an infinite set of exponential models with different growth rates that could be used. While a model fit by means of regression will likely have a reasonable, if not the most probable growth rate, and by extension exclude most other exponential fits as likely to explain the data, this can be difficult to determine. Nonetheless, while there are limitations to this methodology, combining the SPD with a Monte Carlo approach does represent a reasonable starting point for the analysis of the data as long as the substantive interpretation of the findings remain conservative (Crema, 2022; Timpson et al., 2021).

3 Methods and data

Sites surveyed by means of test-pitting between Horten and Arendal were initially retrieved from the national heritage database Askeladden (Norwegian Directorate for Cultural Heritage, 2018), totalling at 1299 records. Any sites situated higher than the marine limit, the highest elevation that the sea reached after the end of the last Ice Age, were then excluded. The remaining records were then manually reviewed and given a quality score based on the criteria in Table 1, indicating the degree to which the spatial location and extent of the sites is believed to be represented in the geometries available in the database (see also Roalkvam, 2020). All sites with a quality score of 4 or worse were excluded from further analysis. Data on excavated sites was originally compiled for Roalkvam (2022) and has been compared with site data as listed in Damlien et al. (2021) and (**nielsen2022?**). Only excavated sites with available spatial data in Askeladden or local databases at the Museum of Cultural History of the University of Oslo were included in the analysis. The 102 excavated sites that have previously been shoreline dated were included in the SSPD along with the retained surveyed sites, giving a total of 934 shoreline dated sites in the SSPD. The borders of the municipalities where the shoreline dated sites are located were used to limit the radiocarbon sample. Radiocarbon dates were taken from Roalkvam (2022) and (**solheim?**). Dates done on food crusts were excluded due an issue with marine reservoir effects (Nielsen et al., 2019, p. 83).

All analyses done in this study were performed using the R programming language (R Core Team, 2020). Underlying data and programming code used for the paper is available in an online repository at X. This is structured as a research compendium following Marwick et al. (2018), to allow for reproducibility of the results (Marwick, 2017). In addition to this, the R package *shoredate*, used for performing and handling the shoreline dating of sites within the study area, is actively being developed and was used for the parts of the analysis that deal with shoreline dates (available from https://github.com/isakro/shoredate).

3.1 Summed probability of calibrated radiocarbon dates

Analysis of the ^{14}C-dates were all done using the *rcarbon* package (Crema and Bevan, 2021) for R. To account for investigatory bias that can result from variable sampling intensity between sites, the radiocarbon dates were initially binned and dates were aggregated on a site by site basis if they fell within 200 uncalibrated ^{14}C years of each other. When calibrated, these are summed and normalised to sum to unity before being included in the final RSPD. Individual ^{14}C-dates were not normalised. This follows from a peculiarity in the calibration procedure which can lead the probability mass of a date to sum to more than one (Weninger et al., 2015). As a consequence of this, normalising the dates before summing has been shown to create spurious spikes in the RSPD. All calibration was done using the IntCal20 calibration curve (Reimer et al., 2020).

The resulting RSPD was then subjected to the null-hypothesis testing approach through Monte Carlo simulation, as introduced above (see Shennan et al., 2013"). This works by first fitting a model to the observed RSPD. Here this was an exponential model, fit by means of regression, and a uniform model. A series of individual calendar years are then drawn from this distribution with replacement, the number of which equals
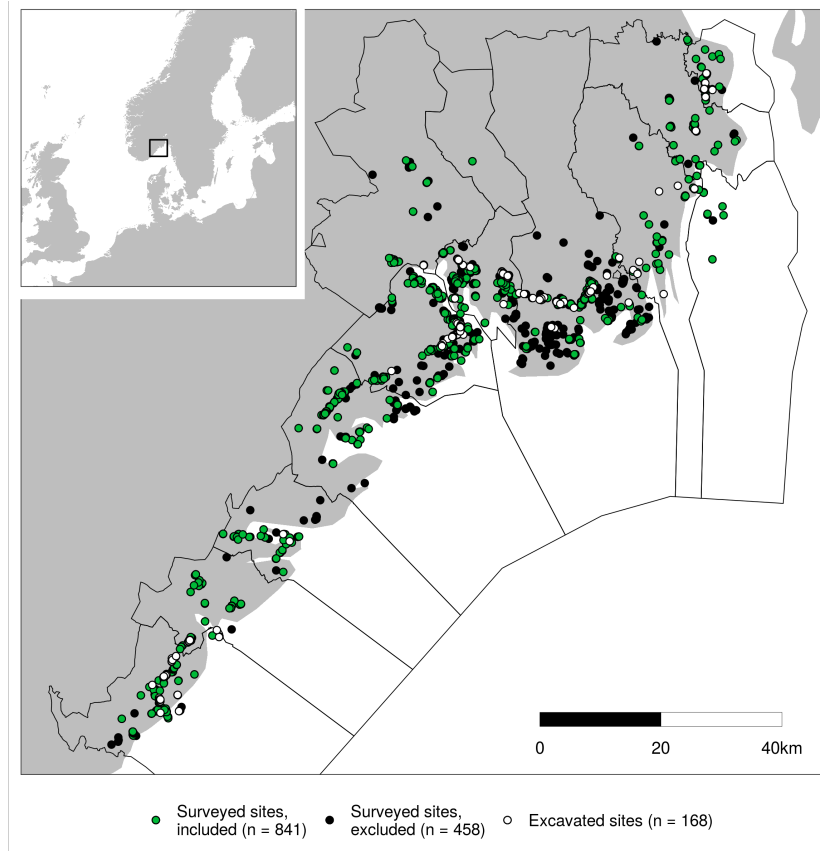
Figure 1: Map of the study area and analysed sites. Black lines indicate the borders between municipalities. The surveyed sites included in the analysis are the ones given a quality score of 3 or better using the framework in Table 1. Of the excavated sites, 102 have been dated by means of shoreline dating.

Table 1: Quality scoring of site records of surveyed sites retrieved from the national heritage database Askeladden. The scoring system was first used in Roalkvam (2020).

Definition	Quality	Count
Site delineated by use of a GNSS-device, or a securely georeferenced record. Extensive database entry.	1	353
Secure spatial data. Slight disturbance of the site or somewhat lacking database record.	2	340
Secure spatial data. Damaged site, such as outskirts of a quarry, and/or very limited database entry.	3	148
Surveyed by archaeologists. However, the database entry is extremely limited/unclear, the site geometry is only given as a point or small automatically generated circle, and/or finds are from the topsoil of a field.	4	165
Likely site but uncertain spatial information. Typical example is recurring stray finds in a field or other larger area.	5	124
Single stray find or unverified claims/suggestions of possible site.	6	169

the number of bins in the observed RSPD. These are then 'uncalibrated' to a single value on the ^{14}C scale and a random error from among the observed errors are added to the date. These are then calibrated back to the calendar scale and finally summed. Here this procedure was repeated 1000 times for each null model. The 2.5th and 97.5th quantile of the resulting summed probability for each year across all simulations were then retrieved to create the 95% critical envelope with which to compare the observed RSPD. The degree to which the observed curve deviates from the critical envelope is then used to calculate a global p-value, indicating whether or not the null model can be rejected.

3.2 Summed probability of shoreline dated sites

Summing the probability of the shoreline dated sites and evaluating the results follows the same structure as that for radiocarbon dates, but idiosyncrasies in the dating method does necessitate some adjustments. First, an illustration of the procedure for shoreline dating a single site, as suggested in Roalkvam (2022), is provided in Figure 2. Four geologic reconstructions of shoreline displacement in the region lays the foundation for the method as implemented here. These shoreline displacement curves are from Horten (Romundset, 2021), Larvik (Sørensen et al., in press, 2014a, 2014b), Tvedestrand (Romundset et al., 2018; Romundset, 2018) and Arendal (Romundset, 2018), each associated with a shoreline isobase along which the trajectory for relative sea-level change has been the same (e.g. Svendsen and Mangerud, 1987). The first step in the dating procedure is therefore to interpolate the shoreline displacement to the location to be dated. This is done by inverse distance weighting (e.g. Conolly, 2020), interpolating the sea-level for each calendar year along the geologic shoreline displacement curves based on the distance from the site to be dated to the isobases of the curves. The likely elevation of the site above the sea-level when it was in use is defined by a function for exponential decay with a decay ratio of 0.168, starting from the elevation of the site (for details see Roalkvam, 2022). This probability is sequentially stepped through at increments of 0.1m and transferred to the calendar year scale by uniformly distributing the probability across each calendar year in the range between the lower and upper limit of the interpolated displacement curve, resulting in the shoreline date. Given that the shoreline displacement curves are monotonic, the shoreline dates are normalised to sum to unity as this should not create spurious spikes in the SSPD (cf. Crema, 2022; Weninger et al., 2015).

In much the same way as characteristics of the calibration curve can introduce bias to the SPD, the same is true for the summed shoreline dates, where the local trajectory of relative sea-level change effectively functions as the calibration curve. As the shoreline displacement curves are interpolated to the sites based on the site location along a south-west–north-east gradient, each site is effectively associated with a unique shoreline displacement curve, provided they are not located on the same isobase. With the analogy to the radiocarbon methodology, this would be equivalent to each date being associated with a unique calibration curve. As it would be computationally prohibitive to interpolate the shoreline displacement trajectory for each date to be simulated in the Monte Carlo procedure, one shoreline displacement curve was initially interpolated to the centre of each of a series of 2km wide line segments running perpendicular to the shoreline gradient between the extremes of the distribution of sites (Figure 3). These intervals were then assigned a probability weight based on how the density of observed sites is distributed among them.

The Monte Carlo simulation then starts by drawing a sample of calendar dates from the observed date range
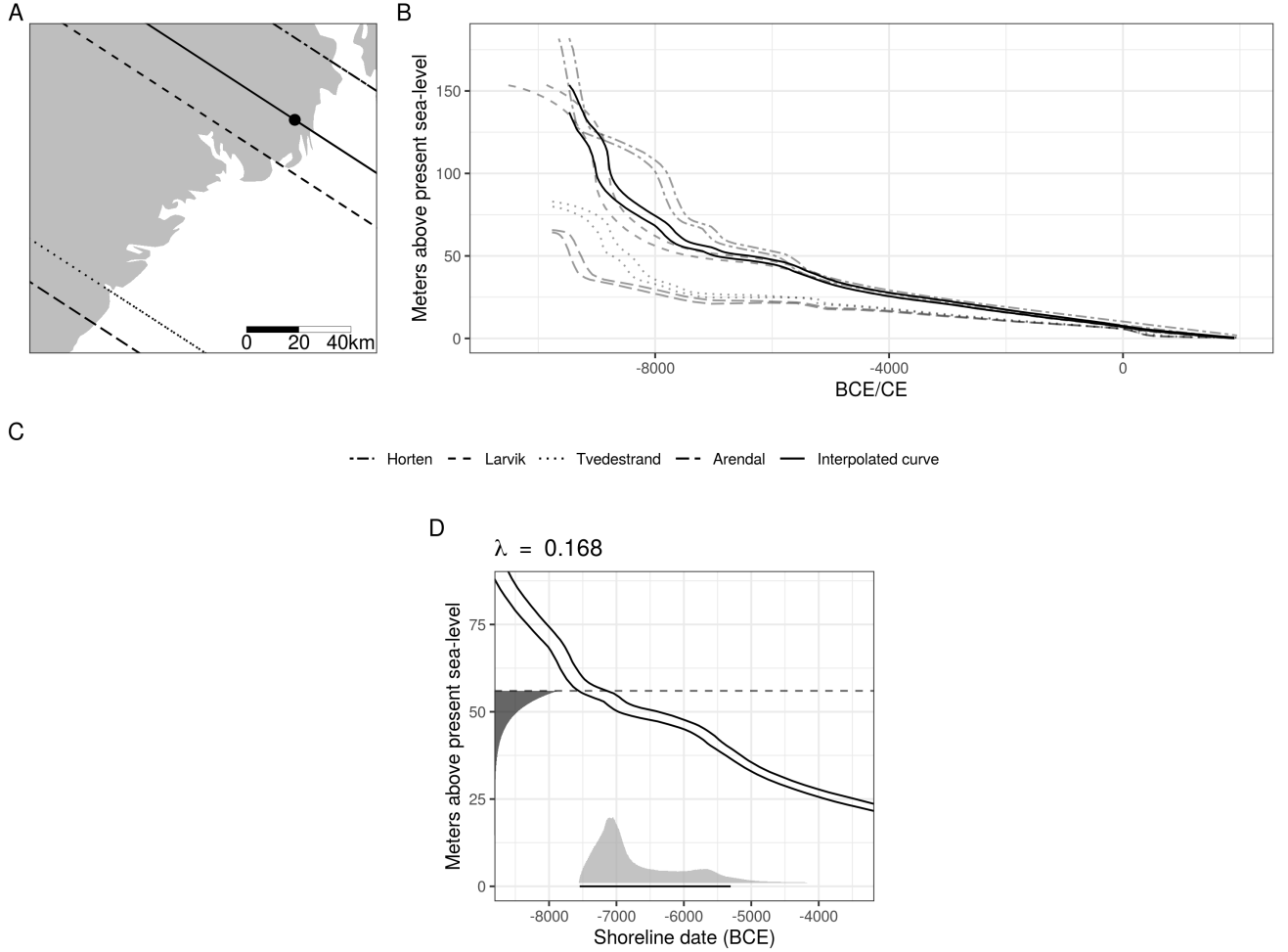
Figure 2: A) Example location relative to the isobases of the displacement curves. B) The geologic displacement curves and the curve interpolated to the example location. C) Resulting shoreline date in light grey on the x-axis. The black line underneath marks the 95% HDR. The dashed line marks the elevation of the example location. The exponential function on the y-axis decays with ratio λ and represents the likely elevation of a site above sea-level when it was in use.
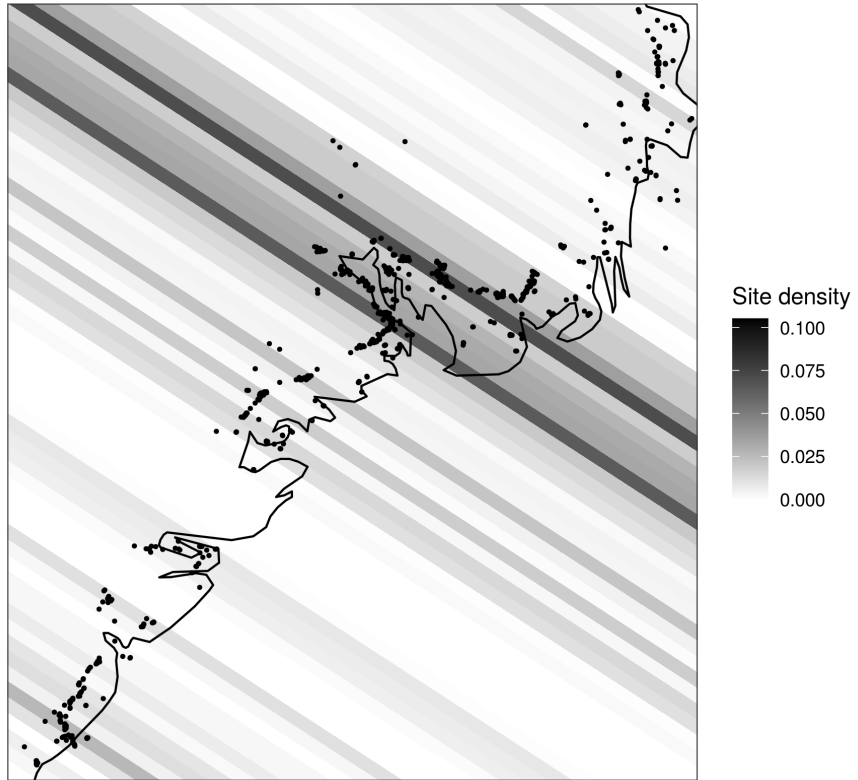
Figure 3: Density of included surveyed sites and excavated sites dated by means of shoreline dating (n = 943) as distributed across the 2km wide line segments that run perpendicular to the shoreline gradient. A displacement curve has been interpolated to the centre of each segment for use in the Monte Carlo simulations below.

in the SSPD, equalling the number of shoreline dated sites, where the probability of drawing any individual year is determined by the null model of choice. Each sampled date is then assigned one of the pre-interpolated displacement curves, the probability of which is weighted by the density of observed sites within each 2km interval. The calendar date is then 'uncalibrated'—to follow the RSPD terminology—to an elevation range from which a single elevation value is then drawn with a uniform probability, using intervals of 5cm. This elevation value is then shoreline dated using the displacement curve for the relevant 2km interval. The dates are then summed, and the process repeated a total of 1000 times. Finally, the 97.5% highest and 2.5% lowest summed probability at each calendar year across all simulations is retrieved to create the 95% critical envelope.
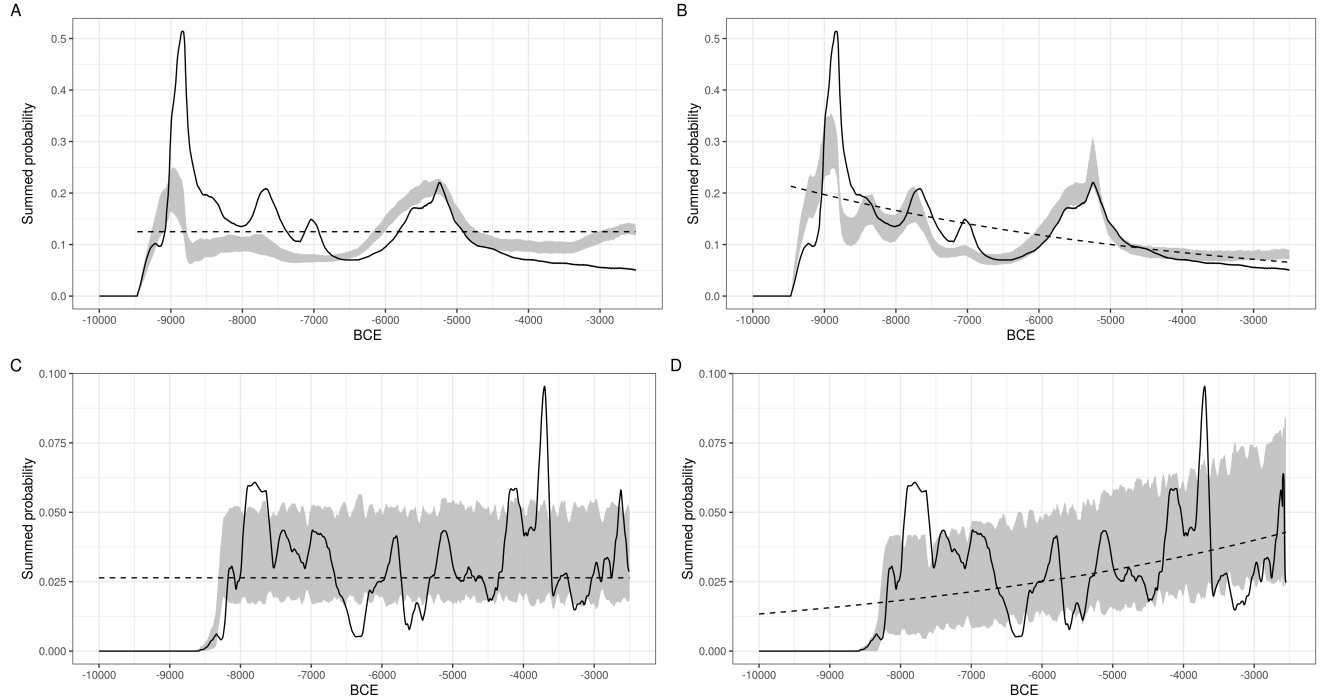
4   Results

Figure 4: [Shoreline sims in this version have only been run 50/1000 times] A) Summed probability of shoreline dated sites (n = 934) compared to a uniform null model. B) Same as A, but with a exponential model. C) Summed probability of calibrated radiocarbon dates (n =, bins = 678) compared to a uniform null model. D) Same as C, but with a exponential null model.

8

5 References

Bergsvik, K.A., Darmark, K., Hjelle, K.L., Aksdal, J., Åstveit, L.I., 2021. Demographic developments in Stone Age coastal western Norway by proxy of radiocarbon dates, stray finds and palynological data. Quaternary Science Reviews 259, 106898. https://doi.org/10.1016/j.quascirev.2021.106898

Blackwell, P.G., Buck, C.E., 2003. The Late Glacial human reoccupation of north-western Europe: new approaches to space-time modelling. Antiquity 77, 232–240. https://doi.org/10.1017/S0003598X00092231

Bluhm, L.E., Surovell, T.A., 2019. Validation of a global model of taphonomic bias using geologic radiocarbon ages. Quaternary Research 91, 325–328. https://doi.org/10.1017/qua.2018.78

Carleton, W.C., Campbell, D., Collard, M., 2018. Radiocarbon dating uncertainty and the reliability of the PEWMA method of time-series analysis for research on long-term human-environment interaction. PloS One 13, e0191055. https://doi.org/10.1371/journal.pone.0191055

Carleton, W.C., Groucutt, H.S., 2021. Sum things are not what they seem: Problems with point-wise interpretations and quantitative analyses of proxies based on aggregated radiocarbon dates. The Holocene 31, 630–643. https://doi.org/10.1177/0959683620981700

Conolly, J., 2020. Spatial interpolation, in: Gillings, M., Hacıgüzeller, P., Lock, G. (Eds.), Archaeological Spatial Analysis: A Methodological Guide. Routledge, London & New York, pp. 118–134.

Crema, E.R., 2022. Statistical inference of prehistoric demography from frequency distributions of radiocarbon dates: a review and a guide for the perplexed. Journal of Archaeological Method and Theory. https://doi.org/10.1007/s10816-022-09559-5

Crema, E.R., Bevan, A., 2021. Inference from large sets of radiocarbon dates: Software and methods. Radiocarbon. https://doi.org/10.1017/RDC.2020.95

Damlien, H., Berg-Hansen, I.M., Melheim, L., Mjærum, A., Persson, P., Schülke, A., Solheim, S., 2021. Steinalderen i Sørøst-Norge: Faglig program for steinalderundersøkelser ved Kulturhistorisk museum. Cappelen Damm Akademisk, Oslo.

Freeman, J., Byers, D.A., Robinson, E., Kelly, R.L., 2018. Culture Process and the Interpretation of Radiocarbon Data. Radiocarbon 60, 453–467. https://doi.org/10.1017/RDC.2017.124

French, J.C., 2016. Demography and the Palaeolithic Archaeological Record. Journal of Archaeological Method and Theory 23, 150–199. https://doi.org/10.1007/s10816-014-9237-4

French, J.C., Riris, P., Fernandéz-López de Pablo, J., Lozano, S., Silva, F., 2021. A manifesto for palaeodemography in the twenty-first century. Philosophical Transactions of the Royal Society B: Biological Sciences 376, 20190707. https://doi.org/10.1098/rstb.2019.0707

Jørgensen, E.K., Pesonen, P., Tallavaara, M., 2020. Climatic changes cause synchronous population dynamics and adaptive strategies among coastal hunter-gatherers in Holocene northern Europe. Quaternary Research 1–16. https://doi.org/10.1017/qua.2019.86

Lundström, V., Robins, P., Riede, F., 2021. Demographic estimates from the Palaeolithic–Mesolithic boundary in Scandinavia: comparative benchmarks and novel insights. Philosophical Transactions of the Royal Society B: Biological Sciences 376, 20200037. https://doi.org/10.1098/rstb.2020.0037

Marwick, B., 2017. Computational Reproducibility in Archaeological Research: Basic Principles and a Case Study of Their Implementation. Journal of Archaeological Method and Theory 24, 424–450. https://doi.org/10.1007/s10816-015-9272-9

Marwick, B., Boettiger, C., Mullen, L., 2018. Packaging Data Analytical Work Reproducibly Using R (and Friends). The American Statistician 72, 80–88. https://doi.org/10.1007/s10816-015-9272-9

Mörner, N.-A., 1979. The Fennoscandian Uplift and Late Cenozoic Geodynamics: Geological Evidence. GeoJournal 3, 287–318. https://doi.org/10.1007/BF00177634

Nielsen, S.V., 2021. A Late Mesolithic Forager Dispersal Caused Pre-Agricultural Demographic Transition in Norway. Oxford Journal of Archaeology 40, 153–175. https://doi.org/https://doi.org/10.1111/ojoa.12218

Nielsen, S.V., Persson, P., Solheim, S., 2019. De-Neolithisation in southern Norway inferred from statistical modelling of radiocarbon dates. Journal of Anthropological Archaeology 53, 82–91. https://doi.org/10.1016/j.jaa.2018.11.004

Norwegian Directorate for Cultural Heritage, 2018. Askeladden versjon 3.0 brukerveiledning.

Palmisano, A., Bevan, A., Shennan, S., 2017. Comparing archaeological proxies for long-term population patterns: An example from central Italy. Journal of Archaeological Science 87, 59–72. https://doi.org/10.1016/j.jas.2017.10.001

R Core Team, 2020. R: A Language and Environment for Statistical Computing. R Foundation for Statistical Computing, Vienna.

Reimer, P.J., Austin, W.E.N., Bard, E., Bayliss, A., Blackwell, P.G., Ramsey, C.B., Butzin, M., Cheng, H., Edwards, R.L., Friedrich, M., Grootes, P.M., Guilderson, T.P., Hajdas, I., Heaton, T.J., Hogg, A.G., Hughen, K.A., Kromer, B., Manning, S.W., Muscheler, R., Palmer, J.G., Pearson, C., Plicht, J. van der, Reimer, R.W., Richards, D.A., Scott, E.M., Southon, J.R., Turney, C.S.M., Wacker, L., Adolphi, F., Büntgen, U., Capano, M., Fahrni, S.M., Fogtmann-Schulz, A., Friedrich, R., Köhler, P., Kudsk, S., Miyake, F., Olsen, J., Reinig, F., Sakamoto, M., Sookdeo, A., Talamo, S., 2020. The IntCal20 Northern Hemisphere Radiocarbon Age Calibration Curve (0–55 cal kBP). Radiocarbon 62, 725–757. https://doi.org/10.1017/RDC.2020.41

Roalkvam, I., 2022. A simulation-based assessment of the relationship between stone age sites and relative sea-level change along the norwegian skagerrak coast. https://doi.org/10.31235/osf.io/3x7ju

Roalkvam, I., 2020. Algorithmic Classification and Statistical Modelling of Coastal Settlement Patterns in Mesolithic South-Eastern Norway. Journal of Computer Applications in Archaeology 3, 288–307. https://doi.org/10.5334/jcaa.60

Romundset, A., 2021. Resultater fra NGUs undersøkelse av etteristidas strandforskyvning nord i Vestfold. Geological Survey of Norway, Trondheim.

Romundset, A., 2018. Postglacial shoreline displacement in the Tvedestrand-Arendal area, in: Reitan, G., Sundström, L. (Eds.), The Stone Age Coastal Settlement in Aust-Agder, Southeast Norway. Cappelen Damm Akademisk, Oslo, pp. 463–478.

Romundset, A., Lakeman, T.R., Høgaas, F., 2018. Quantifying variable rates of postglacial relative sea level fall from a cluster of 24 isolation basins in southern Norway. Quaternary Science Reviews 197, 175–192. https://doi.org/10.1016/j.quascirev.2018.07.041

Shennan, S., 2000. Population, Culture History, and the Dynamics of Culture Change. Current Anthropology 41, 811–835. https://doi.org/10.1086/317403

Shennan, S., Downey, S.S., Timpson, A., Edinborough, K., Colledge, S., Kerig, T., Manning, K., Thomas, M.G., 2013". Regional population collapse followed initial agriculture booms in mid-Holocene Europe. Nature Communications 4, 2486. https://doi.org/10.1038/ncomms3486

Solheim, S., 2020. Mesolithic coastal landscapes. Demography, settlement patterns and subsistence economy in southeastern Norway, in: Schülke, A. (Ed.), Coastal Landscapes of the Mesolithic: Human Engagement with the Coast from the Atlantic to the Baltic Sea. Routledge, London & New York, pp. 44–72.

Solheim, S., Fossum, G., Knutsson, H., 2018. Use-wear analysis of Early Mesolithic flake axes from Southeastern Norway. Journal of Archaeological Science: Reports 17, 560–570. https://doi.org/10.1016/j.jasrep.2017.12.017

Solheim, S., Persson, P., 2018. Early and mid-holocene coastal settlement and demography in southeastern norway: Comparing distribution of radiocarbon dates and shoreline-dated sites, 8500–2000 cal. BCE. Journal of Archaeological Science: Reports 19, 334–343. https://doi.org/10.1016/j.jasrep.2018.03.007

Sørensen, R., Henningsmoen, K.E., Høeg, H.I., Gälman, V., in press. Holocen vegetasjonshistorie og landhevning i søndre Vestfold og sørøstre Telemark, in: Persson, P., Solheim, S. (Eds.), The Stone Age in Telemark. Archaeological results and scientific analysis from Vestfoldbaneprosjektet and E18 Rugtvedt-Dørdal.

Sørensen, R., Henningsmoen, K.E., Høeg, H.I., Gälman, V., 2014a. Holocene landhevningsstudier i søndre vestfold og sørøstre telemark – revidert kurve, in: Melvold, S., Persson, P. (Eds.),. Portal, Kristiansand, pp. 36–47.

Sørensen, R., Høeg, H.I., Henningsmoen, K.E., Skog, G., Labowsky, S.F., Stabell, B., 2014b. Utviklingen av det senglasiale og tidlig preboreale landskapet og vegetasjonen omkring steinalderboplassene ved Pauler, in: Jaksland, L., Persson, P. (Eds.), E18 Brunlanesprosjektet. Bind I. Forutsetninger og kulturhistorisk sammenstilling. University of Oslo, Museum of Cultural History, Oslo, pp. 171–213.

Surovell, T.A., Byrd Finley, J., Smith, G.M., Brantingham, P.J., Kelly, R.L., 2009. Correcting temporal frequency distributions for taphonomic bias. Journal of Archaeological Science 36, 1715–1724. https://doi.org/10.1016/j.jas.2009.03.029

Svendsen, J.I., Mangerud, J., 1987. Late Weichselian and Holocene sea-level history for a cross-section of western Norway. Journal of Quaternary Science 2, 113–132. https://doi.org/10.1002/jqs.3390020205

Tallavaara, M., Pesonen, P., 2020. Human ecodynamics in the north-west coast of Finland 10,000–2000 years

ago. Quaternary International 549, 26–35. https://doi.org/10.1016/j.quaint.2018.06.032

Timpson, A., Barberena, R., Thomas, M.G., Méndez, C., Manning, K., 2021. Directly modelling population dynamics in the South American Arid Diagonal using 14C dates. Philosophical Transactions of the Royal Society B: Biological Sciences 376, 20190723. https://doi.org/10.1098/rstb.2019.0723

Torfing, T., 2015. Neolithic population and summed probability distribution of 14C-dates. Journal of Archaeological Science 63, 193–198. https://doi.org/10.1016/j.jas.2015.06.004

Weninger, B., Clare, L., Jöris, O., Jung, R., Edinborough, K., 2015. Quantum theory of radiocarbon calibration. World Archaeology 47, 543–566. https://doi.org/10.1080/00438243.2015.1064022